JOURNAL OF AGRICULTURAL AND FOOD CHEMISTRY

Crystallization and Polymorphism of Triacylglycerols Contribute to the Rheological Properties of Processed Cheese

HELA GLIGUEM,[†] DORRA GHORBEL,[‡,§] CHRISTELLE LOPEZ,[||] CAMILLE MICHON,[⊥] MICHEL OLLIVON,[†,#] AND PIERRE LESIEUR*,[▽]

Equipe Physico-Chimie des Systèmes Polyphasés, UMR 8612 du CNRS, 5 rue J. B. Clément, 92296 Châtenay-Malabry, France, Unité d'Analyses Alimentaires, ENIS, BPW 3038 Sfax, Tunisia, Département de Génie Biologique et Chimique, INSAT, Centre Urbain Nord, B.P. 676, 1080, Tunis, Tunisia, UMR 1253 Science et Technologie du Lait et de l'Oeuf, INRA-Agrocampus Rennes, 65 rue de Saint-Brieuc, 35042 Rennes cedex, France, Laboratoire de Biophysique des Matériaux Alimentaires, UMR SCALE 1211, AgroParisTech, 1 avenue des Olympiades, 91744 Massy, France, and Faculté des Sciences, Université Henri Poincaré, UMR 7565, 54506 Vandœuvre-lès-Nancy cedex, France

The thermal, rheological, and structural behaviors of a spreadable processed cheese were studied by complementary techniques including differential scanning calorimetry (DSC), rheology, and X-ray diffraction as a function of temperature. In this product, fat is present as a dispersed phase. Thermal and rheological properties were studied at different cooling rates between 0.5 and 10 °C min^{-1} from 60 to 3 °C. Crystallization properties of fat were monitored at a cooling rate of −2 °C min^{-1} from 60 to −10 °C. Fat triacylglycerols (TGs) crystallized at 15 °C in a triple-chain length 3Lα (72 Å) structure correlated to exothermic events and to the sudden increase in the rheological moduli G' and G''. Upon heating at 2 °C min^{-1}, the polymorphic transition of TGs evidence the melting of the 3Lα structure and the formation of a 2Lβ' (36.7−41.5 Å) structure. Melting of the latter follows. These transformations coincide with thermal events observed by DSC and the decrease in two steps of the rheological moduli. The influence of fat crystallization, melting, and polymorphism upon the viscoelastic properties is clearly demonstrated upon both heating and cooling.

KEYWORDS: Processed cheese; fat; rheology; differential scanning calorimetry; X-ray diffraction

INTRODUCTION

Processed cheeses are very popular in many countries and have therefore a considerable economic importance. They have a long shelf life (>6 months) as compared to other cheeses, since they are stable from a microbiological point of view. Different kinds of processed cheeses exist as follows: slices, blocks, or spreads. Because of its spreadability, processed cheese requires a more delicate monitoring of the product texture.

In the processed cheeses, fat is generally of dairy origin. Milk fat is mainly composed of a great variety of triacylglycerols (TGs; esters of glycerol and fatty acids) in which the fatty acids vary in chain length and unsaturation (*1*). The TG composition induces a complex crystallization behavior and a melting range that spans from about −40 to 40 °C with multiple melting points (*2*). Furthermore, individual TGs are characterized by a complex thermal behavior in relation with their polymorphism of monotropic type (*3*).

The texture of processed cheese is a very important parameter affecting the acceptability of the product by the consumer. Both microstructure (*4*) and rheological properties (*5*) of spreadable processed cheese formulas are strongly dependent on the properties of fat. The dispersion state of milk fat, in either globular or anhydrous form, has an effect on both its thermal and its structural properties (*6*−*8*). In cheeses, the distribution of fat within the protein matrix is an essential component of the cheese texture. Its knowledge helps in understanding the functional properties. Characterizing the cheese microstructure, particularly the fat dispersion within the matrix, is possible using microscopy methods (*4, 9, 10*).

In physical terms, processed cheese spread is a viscoelastic material. Although the fat phase of most cheeses may be crystallized at the temperature of storage and consumption, the most widely functional properties investigated in cheese industry are characterized only during heating. The viscoelastic properties

* To whom correspondence should be addressed. Fax: +33 1 46 83 53 12. E-mail: pierre.lesieur@uhp-nancy.fr.
[†] UMR 8612 du CNRS.
[‡] ENIS.
[§] INSAT.
[||] INRA-Agrocampus Rennes.
[⊥] UMR SCALE 1211.
[#] This work was initiated by Michel Ollivon, who passed away June 16, 2007.
[▽] UMR 7565.

10.1021/jf802956b CCC: $40.75
Published on Web 03/18/2009

of processed cheeses were considered on either heating (*11*) or heating followed by subsequent cooling (*5*). However, they were not considered on cooling followed by subsequent heating, although this allows one to focus on the physical properties of processed cheeses in relation to their fat fraction thermal behavior. Dynamic rheological testing upon heating temperature sweeps is a powerful way to characterize melting properties of cheeses as it can be carried out in nondestructive deformation conditions (*12*, *13*).

Earlier, X-ray diffraction (XRD) was applied to cheddar cheese to follow changes that may occur during ripening. The study was focused on the cheese protein fraction (*14*). Thereafter, Evans and Pillinger (*15*) were interested in both the protein and the fat fractions of cheddar cheese. They observed by X-ray crystallography crystalline structures formed by TGs and by amino acids. Recently, Lopez et al. (*16*) identified the crystalline structures formed by TGs in emmental cheeses stored at 4 °C. With regard to processed cheeses, XRD was used years ago only to investigate, in situ, crystals in the aqueous phase such as calcium citrate, lactose, dicalcium phosphate, disodium phosphate, melting salts, or tyrosine (*17*, *18*).

Differential scanning calorimetry (DSC) and XRD were used to characterize thermal and structural properties of milk fat, respectively. DSC is a useful tool to determine the melting and crystallization temperatures of fat, as well as to follow its polymorphic evolutions. It was commonly used to study the polymorphism of milk fat in bulk and in emulsions (*6*, *19*). Even if most cheeses are fat-rich products, studies of the polymorphism of the fat phase dispersed in cheese by DSC are scarce. A recent study was performed on emmental cheese by Lopez et al. (*20*, *21*). DSC was used to monitor the thermal properties and polymorphic evolutions of fat after the main stages of manufacturing and ripening of emmental cheese (*22*, *23*) and mozzarella cheese (*24*). XRD allows the characterization of fat structures in the crystalline state (*25*). XRD coupled to differential thermal analysis (DTA) allowed the study of fat in either the anhydrous state (*8*, *19*) or dispersed as an emulsion (*6*, *7*, *26*).

The objective of this work was to investigate, over a wide temperature range, the structural and thermal behaviors of the fat fraction and to relate them to the small deformation rheological properties of processed cheese. As will be shown, the used techniques form a promising combination of techniques to relate the viscoelastic properties to the polymorphism of TGs in processed cheeses.

MATERIALS AND METHODS

Samples. Processed cheese samples were provided by a French dairy company (Fromageries Bel, Vendôme, France). All of the samples analyzed in this study were produced from the same batch to avoid any differences in their chemical composition and in their microstructure organization. The samples were stored at +4 °C prior to analysis.

Physicochemical Analysis. Processed cheese was analyzed for dry matter, fat content, total nitrogen expressed as protein content, lactose, and ash contents. The pH of the cheese was also measured. All analyses were performed in triplicate. The studied processed cheese was characterized by a dry matter content of 43.30 ± 0.15% (w/w), a fat in dry matter content of 52.00 ± 0.21% (w/w), a total protein content of 10.50 ± 0.11% (w/w), and a pH value of 5.52 ± 0.01. Lactose and ash contents were 6.80 ± 0.07 (w/w) and 3.70 ± 0.01% (w/w), respectively.

Dynamic Rheological Measurements. The rheological experiments were performed using a controlled-stress rheometer (Carri-Med CSL^2 100, T.A. Instruments, France), fitted with a ridged parallel plate (40 mm in diameter) measuring tool. The use of the ridged plates prevented specimen slippage. To prevent dehydration of the sample during the test, the rheometer was fitted with a moisture trap. Cooling and heating ramps were performed through the lower plate using a Peltier plate that provided very accurate temperature control. For each temperature sweep, the effective temperature in the gap was measured by using a thermocouple. Temperature sweeps were performed from 70 down to 3 °C at the slow and intermediate cooling rates of −0.5, −1, and −2 °C min^{-1}, then from 3 up to 60 or 70 at 2 °C min^{-1}. Faster cooling conditions were also applied and followed by heating at the same rate. However, because of the cooling regulation limits, −5 and −10 °C min^{-1} rates could not be obtained as for DSC experiments (see below). Temperature sweeps were then performed at the cooling rates of −4 and −6.5 °C min^{-1}. Specimens of 40 mm in diameter and 2 mm in height were cut at +4 °C by using a cylindrical tube and placed manually onto the lower plate surface. The lower plate was then raised to the measuring position with a gap of 2 mm. Sample excess was removed from the edges of the measuring tool using a circular plastic spatula. Before each experiment, samples were equilibrated at a temperature of 70 °C for 2 min between the ridged plates. Measurements were performed in the linear viscoelastic region (determined by preliminary experiments at 4, 25, and 70 °C) by applying a constant strain of 0.1% and a constant frequency of 1 rad s^{-1}. The rheological parameters, G' (storage modulus, Pa) and G'' (loss modulus, Pa), were recorded in triplicate vs temperature.

DSC Experiments. DSC experiments were carried out using a Perkin-Elmer DSC-7 apparatus (St. Quentin en Yvelines, France) supported by a Pyris Thermal Analyzing System (version 3.52). Dried nitrogen and air were used to purge the thermal analysis system (head and glovebox, respectively) during all experiments. Lauric acid (99.95% purity, melting point = 43.7 °C; $\Delta H_{melting}$ = 36.8 kJ mol^{-1}) was used as a standard to calibrate the calorimeter for all cooling and heating rates applied. The cheeses samples, in the range of 10−15 mg, were first hermetically sealed into 40 μL aluminum pans (pan, part BO14-3021, and cover, part BO14-3004). An empty pan was used as a reference. The samples were cooled from 60 to 3 °C at different rates, $|dT/dt|$ = 0.5, 1, 2, 5, and 10 °C min^{-1}, then heated from 3 to 60 °C at the constant rate, dT/dt = 2 °C min^{-1}. DSC sample analyses were performed in triplicate with excellent repeatability. Only one thermogram will be presented in the paper.

Combined X-rays and DTA Measurements. XRD was performed using the small-angle X-ray scattering beamline of synchrotron Elettra (Trieste, Italy) at 8 keV, λ = 1.54 Å. Two linear detectors (1024 channels each) were located at small (SAXD) and wide (WAXD) angles for XRD data collection. The cell of the calorimeter "Microcalix" (see details in Ollivon et al., ref *27*), was positioned perpendicular to the X-ray beam, to allow the recording of XRD as a function of temperature (XRDT) and the coupling with DTA experiments (*6*).

Calibration of the X-ray detectors was carried out at small angles using silver behenate (d_{001} = 58.38 Å) and at wide angles with pure β-tristearin (d = 3.70, 3.85 and 4.59 Å) at room temperature. The results are expressed using the scattering vector ($q = 4\pi.\sin\theta/\lambda$; q in Å^{-1}, θ is the incidence angle of the X-rays relatively to the crystalline plane, and λ is the X-ray wavelength). All XRD patterns were recorded by transmission using glass capillaries (diameter, 1.5 mm; wall thickness, 0.01 mm) (GLAS W. Muller, Berlin, Germany). A processed cheese sample was filled into the capillary, at 4 °C, using a laboratory-made syringe. The capillary was transferred at 60 °C into the calorimeter preheated to the same temperature to eliminate all thermal history of the processed cheese sample. Then, the samples were cooled from 60 to −10 °C at $|dT/dt|$ = 2 °C min^{-1} and heated from −10 to 60 °C at dT/dt = 2 °C min^{-1}. Simple analysis of the XRD patterns recorded as a function of time was performed by using IGOR PRO 4.0 Software (Wavemetrics, Portland, United States). For more detailed analysis, each XRD pattern, recorded either upon cooling or upon heating, was analyzed by using PEAKFIT software (Jandel Scientific, Erkrath, Germany). Each peak of the XRD pattern was fitted by the sum of a Gaussian and a Lorentzian function with identical central positions and half-width at half-maximum, the relative weight of these two functions being a shape parameter. The area, the maximal intensity, and the position of the maximum were thus obtained for each peak of the XRD patterns (see Lopez et al., ref *6*).

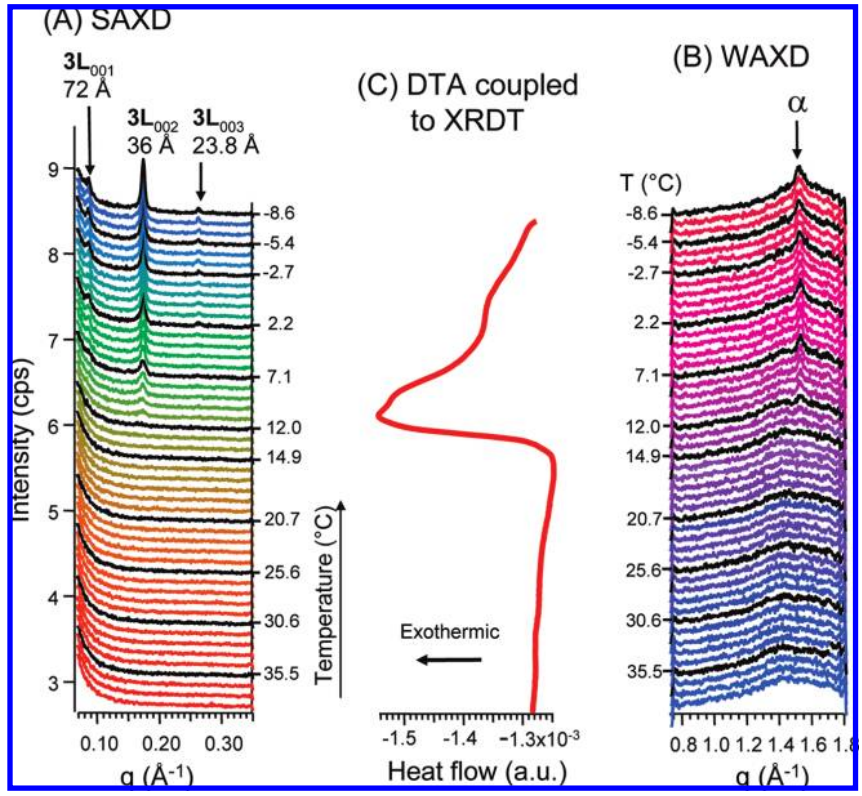

Figure 1. Coupled XRD and DTA scans recorded during cooling of processed cheese from 60 to −10 °C at −2 °C min^{-1}. Frames between 60 and 39 °C have not been reproduced.

RESULTS AND DISCUSSION

Physical Properties of Processed Cheese on Cooling. *Crystallization Properties of Fat in Processed Cheese.* The crystallization properties of TGs dispersed in the processed cheese were monitored using XRD, on cooling at −2 °C min^{-1}. The X-ray patterns recorded at small and wide angles during cooling are presented in **Figure 1A**,**B**, respectively) together with the DTA curve recorded simultaneously on the same sample (**Figure 1C**).

X-ray patterns demonstrate two temperature-delimited domains. Above 14.5 °C, TGs are in their liquid state, as confirmed by DTA recording (**Figure 1C**). At small angles, no diffraction line is recorded, and at wide angles, the X-ray bump recorded at $q = 1.40$ Å^{-1} (4.5 Å) is related to scattering from the liquid organization of TGs (*28*). For $T \leq 14.5$ °C, the diffraction lines at small and wide angles correspond to the formation of a crystalline structure with a triple-chain length stacking of TGs known as 3L with a repeat distance of 72 Å ($3L_{002}$, 36 Å; $3L_{003}$, 23.8 Å). TGs with both short and long chains or with an unsaturation are known to form such 3L structures (*29*). At wide angles, the single diffraction peak recorded at $q = 1.514$ Å^{-1} (4.15 Å) is characteristic of a hexagonal packing (unstable α form) of the alkyl chains. The diffraction lines intensities increase upon cooling below 14.5 °C. So, only a partial and progressive crystallization occurs as a liquid → 3Lα (72 Å) transition.

Below 14.5 °C, the fat matter in the processed cheese droplets (0.7 μm in average diameter, result not shown) is a mixture of the liquid and the solid phases of TGs. Our result is consistent with previous observations stating that crystallization in milk fat globules (4 μm in diameter) gives rise to a 2Lα (42−47 Å) structure followed by a 3Lα (71.2 Å) one, while in fat droplets ranging from 1.25 to 0.38 μm, only the 3Lα (72 Å) is observed (*7*). Thus, the crystallization in the 3Lα (72 Å) form characterized in processed cheese may be related to the small size of fat droplets (0.7 μm).

The comparison of the X-ray and DTA data allows us to relate the structural changes to the thermal events observed, as indicated in **Figure 1**. The crystallization curve shows a global exothermic process of crystallization with an onset temperature, T_{onset}, of 14.5 °C. This onset is slightly lower than the one recorded with the DSC-7 (15.1 ± 0.1 °C) for the sample cooled at the same rate of 2 °C min^{-1} (see **Table 1**).

Thermal Properties of Fat in Processed Cheese. The thermal properties of processed cheese (**Figure 2A**) were studied by DSC-7 at different cooling rates between −0.5 and −10 °C min^{-1}. The exothermic peaks recorded on cooling were only related to the crystallization of TGs in the fat droplets since caseins do not exhibit thermal transitions in the temperature region investigated (*30*). DSC-7 experiments allowed the recording of the phase transition from the liquid to the solid state of TGs in the processed cheese. The onset temperature of crystallization and the shape of the crystallization curves depend on the cooling rate (**Figure 2A**). At least two exothermic events were always recorded on cooling. The faster the cooling rate was, the lower the crystallization temperatures of the two thermal events (**Table 1**) were. This temperature shift may be related to the kinetics of the crystallization process and to the nucleation rate in the dispersed phase of the processed cheese, as previously discussed in Lopez et al. (*7*). When crystallization takes place in a relatively short period of time, mixed crystals are formed. This is consistent with the peak broadening observed upon a cooling rate increase. Such a result was also evidenced on the thermal behavior of cream (*7*) and anhydrous milk fat (*8*, *31*).

Viscoelastic Properties of Processed Cheese. Small deformation rheology gives access to the storage and loss moduli, G' and G'', which are plotted against temperature, from 60 to 3

Table 1. Crystallization Onset Temperature (DSC-7 Measurements) and Threshold Temperatures for G' Increase upon Fat Crystallization and Final Melting Temperature (DSC-7)[a]

cooling rate [dT/dt (°C min^{-1})]	−0.5	−1	−2	−5	−10
onset temperature of crystallization (°C)	15.4 ± 0.4	15.1 ± 0.2	15.1 ± 0.1	13.9 ± 0.2	13.6 ± 0.4
CV (%)	2.6	1.4	0.7	1.1	3.0
threshold temperature for G' increase	13.4 ± 0.2	13.3 ± 0.3	13.2 ± 0.2	13.2 ± 0.2[b]	13.0 ± 0.4[c]
CV (%)	1.1	2.3	1.6	1.5	2.8
final melting temperature (°C)	38.4 ± 0.3	38.2 ± 0.1	38.2 ± 0.2	38.5 ± 0.1	38.3 ± 0.1
CV (%)	0.7	0.3	0.5	0.2	0.2

[a] Cooling was performed at the indicated rates and melting at 2 °C min^{-1} (mean values ± standard deviations from three independent experiments). CV, coefficient of variation. [b] The cooling rate was −4 °C min^{-1}. [c] The cooling rate was −6.5 °C min^{-1}.

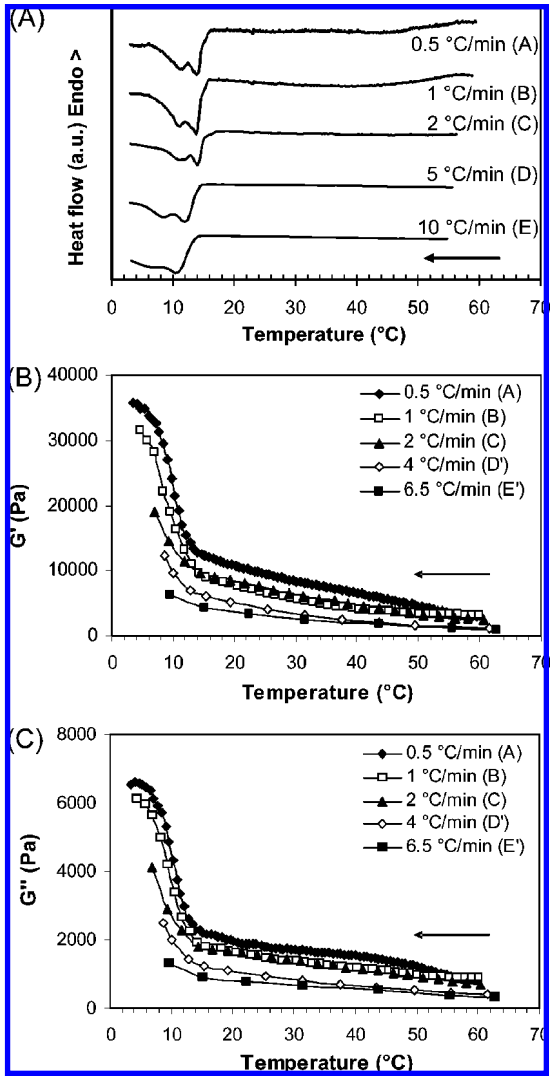

Figure 2. Influence of cooling rate on thermal and viscoelastic properties of processed cheese. (**A**) DSC crystallization curves were recorded in the same conditions. (**B** and **C**) Variations of G' and G'' vs temperature and recorded at different cooling rates are as indicated in the figure. High cooling rates are slightly different for the two techniques due to limitations of the technology used for rheological measurements.

°C, at different cooling rates in **Figure 2B**,**C**. Over the whole temperature interval of the study, the processed cheese presents high G' values and a low G''/G' ratio (0.15 to 0.35) characteristic of a viscoelastic gel. Besides, upon cooling, the G' and G'' moduli increase with decreasing temperature whatever the cooling rate. The weakest values of G' and G'' were recorded at high temperature, for example, 60 °C. They are the result of a smaller number of links between casein aggregates, the liquid state of fat, and thermal agitation.

For $T < 50$ °C and for slow (0.5 °C min^{-1}) and intermediate (1 and 2 °C min^{-1}) cooling rates, G' and G'' increase slowly upon a temperature decrease down to 13 °C; they then very sharply rise up (**Figure 2** and **Table 1**). Between 13 and 3 °C, G' and G'' are multiplied by a factor of 2−3. This reinforcement of the dynamic moduli is related to a more solidlike behavior and to fat crystallization. For the fastest cooling rates (4 and 6.5 °C min^{-1}), the G' and G'' curves display similar shapes with, however, a much lower increase in the rheological moduli.

Larger storage and loss moduli (and thus elastic and viscous components) were obtained with lower cooling rates. This is in good agreement with the observations performed by other authors on protein gels (that constitute the continuous medium of processed cheeses), rennet casein systems, or during industrial observations (*32*). Similar results were reported by other researchers for processed cheeses (*33*, *34*). Caric and Kalab (*35*) showed that a slower cooling process yields to a firmer processed cheese. However, the cooling effects have not been fully explained. More recently, Piska and Stetina (*36*) found that a rapid cooling of the molten mass has an influence on the texture and rheological properties of processed cheese as a rapid cooling leads to a decrease of the rigidity of the product expressed in terms of rheological parameters (complex modulus, yield stress) and also in terms of textural ones (hardness, gumminess).

Relation between the Crystallization Properties of Fat and the Viscoelastic Properties of Processed Cheese. To better correlate the X-ray data with the rheological results, the intensities of the SAXD lines have been determined through the detailed analysis of the individual frames. Each line intensity was expressed as the percentage of its maximal value observed in the temperature interval of the study as reported in **Figure 3A**.

The intensities of the three SAXD lines have nearly indistinguishable variations upon cooling. A linear increase is first observed below 15 °C. Then, the intensities saturate and reach their maximum at the lowest temperature of the measurements.

The DTA signal measured simultaneously with the X-ray patterns has been reproduced in **Figure 3B**. Its cumulative integration relative to the extrapolated baseline is also depicted in **Figure 3B**. Its variations are similar to those of the SAXD intensities, and the two major exotherms, at 12 and 9.5 °C, can probably be attributed to the formation of the 3Lα (72 Å) crystals in the fat droplets. Because of its low intensity, the very small exotherm near 0 °C will not be considered. The presence of two exotherms associated with the same crystalline structure, although astonishing, might be due to the polydispersity in size and composition of the fat droplets. Before the crystallization occurs in a given droplet, the liquid fat is in the

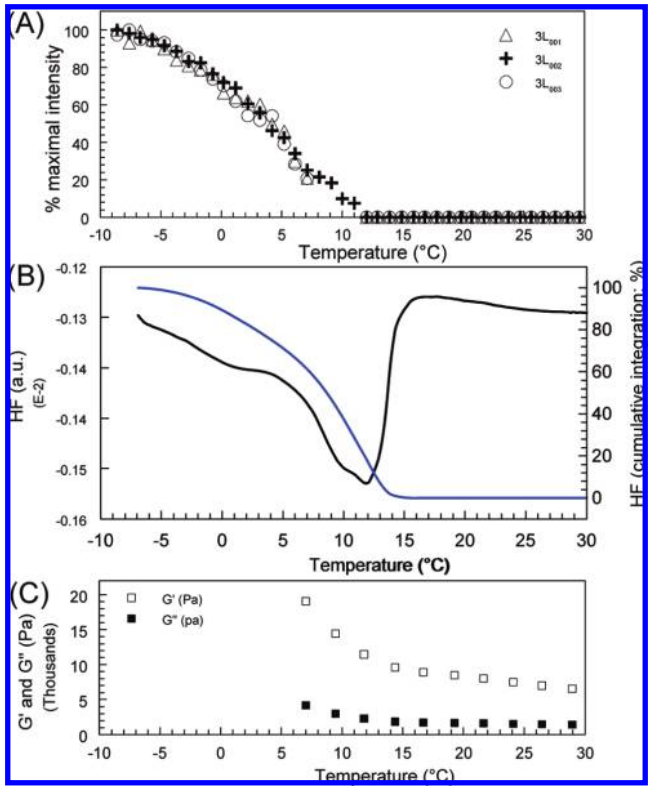

Figure 3. (**A**) Evolution of the maximal intensities of the SAXD peaks recorded upon cooling of the processed cheese at −2 °C min^{-1}. (**B**) DTA heat flow and its cumulative integration as a function of temperature. (**C**) Evolution of G' and G'' on cooling at −2 °C min^{-1}.

supercooled state and the phase change might be influenced by the proximity or the nature of the surrounding membrane composed of different kinds of proteins. The presence of these two thermal events and the spreading of the transition over a temperature interval of about 25 °C (from 15 to −10 °C) are finally a reasonable behavior for such a complex system.

The behaviors of the viscoelastic moduli G' and G'' are reproduced on **Figure 3C**. The change in their behavior with a faster increase below 13.5 °C is clearly related to the crystallization of the 3Lα (72 Å). Certainly, fat crystallization reinforces the proteins anchorage onto the droplets and thus contributes to the firmness of the cheese at low temperatures. Hence, crystallization of the fat fraction of processed cheese is responsible for the G' and G'' increase that occurs in the temperature domain 13 → 3 °C. However, a slight difference ($\Delta T \sim 2$ °C) is observed between the initial temperatures given by rheometry and calorimetric techniques (**Table 1**). Probably, a sufficiently large number of fat crystals must be present to modify the rheological properties of the processed cheese. This can only occur at a temperature lower than the onset one measured on the DSC-7 curves. Furthermore, the rheological measurements were performed under shear, whereas static conditions were used for the DSC-7 recordings. The former ones occur in the linear harmonic regime so that the small deformation of the cheese should not affect the physical properties of the processed cheese concerning both the crystallization of fat in the droplets and the continuous phase. Upon cooling, above 14 °C, the fat fraction remains in the liquid state. The G' and G'' moduli variations, between 50 and 14 °C, can be attributed to the protein fraction through the increase of hydrophobic links, hydrogen bonds, or other temperature sensitive cross-links (*37*). Finally, the increase of G' and G'' between 60 and 3 °C seems to be the result of two cumulative phenomena: first, the reinforcement of the protein matrix, and second, the crystallization of TGs in the fat droplets.

Physical Properties of Processed Cheese on Heating. *Melting Properties and Polymorphism of Fat in Processed Cheese.* Coupled XRDT/DTA experiments recorded while heating the processed cheese sample are plotted in **Figure 4**. Small angle XRD patterns (**Figure 4A**) could be divided in four temperature-delimited domains. In the first one, from −10 to 14 °C, the three diffraction lines previously formed on cooling at −2 °C min^{-1} and related to the 3L (72 Å) decreased in intensity. Then, in the $11 \leq T \leq 15$ °C domain, the broadening of the line observed at 36 Å was attributed to the melting of the well-structured 3L crystallites and the presence or growth of a double chain length 2L (36.7 Å) structure. It would be simpler to consider that the 3L phase remains, as a less or ill ordered structure, above 11 °C and up to 15 or 20 °C. However, the continuous shift of the peak position from 11 to 20 °C suggests and has led us to consider a 2L structure as depicted above. So, the diffraction line near 0.17 Å^{-1} corresponds to both the second order diffraction line of the 3L structure ($3L_{002}$) and the first order line of the 2L (36.7 Å) structure.

Simultaneously, at wide angles, the decrease in intensity of the characteristic peak of the α form was observed (**Figure 4B**). These structural changes are related to the melting of the 3Lα (72 Å) structure. The two diffraction peaks at about 3.9 and 4.2 Å characteristic of the formation of a β' crystalline form could hardly be detected.

Transformation of the later 2L phase is observed up to 20−22 °C. At small angles, a continuous increase of its repeat distance is observed from $d = 36.7$ Å at $T = 14$ °C to 40.6 Å at $T = 22$ °C. At wide angles, no characteristic peak can be extracted from the data due to the low signal/noise ratio, although the 2L phase is probably of the β' type (*6*). At higher temperatures (22 to 38−40 °C), the period of the 2Lβ' structure remains nearly constant (small variations from 40.6 to 41.5 Å), while its melting is observed from the progressive lowering of the SAXD line and the simultaneous endotherm shown by the coupled calorimetric data. From this offset temperature and up to 60 °C, no diffraction line is observed, and the TGs remain in the liquid state.

DTA (**Figure 4C**) and DSC-7 (see **Figures 5A** and **6**) thermograms demonstrate the same endotherms except the small endotherm between 21 and 25 °C, observed only with the DSC-7 apparatus. A first endotherm, at $T \leq 10$ °C, appears as a shoulder since, up to 5 °C, the broad signal observed is associated with the calorimeter equilibration. The correlation between XRD and DTA data shows that this first thermal event is attributed to the melting of the unstable 3Lα (72 Å) form. The exothermic event, well seen between about 10 and 13 °C with the DSC-7 (see **Figure 5A**), remains hardly visible with the coupled DTA instrument. Nevertheless, it is associated to the balance of the 3L (72 Å) melting and the 2L (36.7 Å) formation as observed with SAXD. Such rearrangements of the TGs molecules into a lamellar organization are facilitated by the presence of a liquid phase due to the melting of the 3L (72 Å) variety (*8*). The second endotherm, from 14 to 23 °C (13−21 °C with the DSC-7), corresponds to a noticeable increase of the long spacing from 36.7 to 40.6 Å and thus to a rearrangement of TGs, which leads to the formation of a more stable 2L structure. A diffraction peak at small angles is still visible, while no peak is present in the WAXD patterns due to the low signal/noise ratio. The third and broad melting endotherm (the third and fourth observed with the DSC-7) (from 23 to 40.3 °C here and from 21 to 38

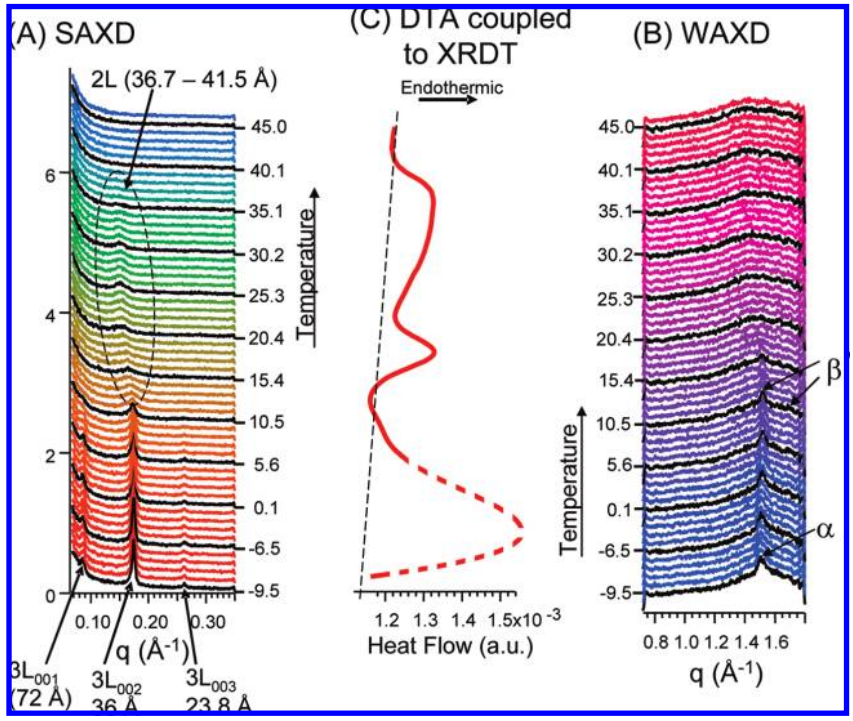

Figure 4. Coupled XRD and DTA scans recorded during subsequent heating of processed cheese at 2 °C min^{-1}.

°C with the DSC-7) corresponds to the progressive melting of the 2L structure.

To conclude, the coupled SAXD, WAXD, and DTA measurements lead upon heating to the following transitions of the TGs in the fat droplets:

$$3L\alpha(72\ \text{Å}) \xrightarrow{3-13\ °C} 2L(36.7\ \text{Å}) \xrightarrow{13-25\ °C}$$

$$2L\beta'(40.6\ \text{Å}) \xrightarrow{25-38\ °C} \text{liquid}$$

Thermal Properties of Fat on Heating. The DSC-7 melting curves recorded upon heating of processed cheese at 2 °C min^{-1} after the samples were cooled down at different rates varying from −0.5 to −10 °C min^{-1} are shown in **Figure 5A**. All of the recordings show three partially individualized endotherms. Besides, an endotherm is known to occur below 6 °C (data not shown). A small exothermic event follows between 6 and 12 °C. These two thermal events partly compensate for each other, and the exotherm is more clearly evidenced at slow cooling rates.

The second endotherm was recorded between approximately 10−13 and 20−21 °C. The endothermic character of the transition might let us consider a simple melting transformation. However, in this temperature interval, the newly formed 2L structure has a highly varying repeat distance but does not seem to grow or melt. Melting of short period structures and thus TGs with short chains might occur together with crystallization of longer TGs.

The third and small endotherm was recorded between 21 and 25 °C. It is mainly observable for precooling rates of 2 and 4 °C min^{-1}.

The fourth and broad endotherm was recorded from 25 °C until the final melting of TGs is observed at an offset temperature between 38.1 and 38.5 °C (**Table 1**). Roughly, the final melting point of processed cheese fat can be considered as independent of the cooling rate, as it is the case for cream studied under similar conditions (*7*).

Viscoelastic Properties of Processed Cheese. After having been cooled down at different rates, the processed cheese samples were heated at the same rate of 2 °C min^{-1}. Rheological measurements (**Figure 5B**,**C**) were performed under similar experimental conditions as DSC-7 ones.

The values of both parameters G' and G'' at 3 °C (**Figure 5B**,**C**) are higher than those observed at the end of the cooling. According to the protocol used, the processed cheese was maintained during 2 min at 3 °C. During this short period, more strengthening links are certainly formed in the processed cheese, which although already structured upon cooling, thus becomes an even more structured product. Upon heating, the curves of G' and G'' vs temperature present similar shapes whatever the previous cooling rate applied. As shown in **Figure 5B**,**C**, the G' and G'' curves display a large decrease from 3 to about 21 °C followed by a small shoulder; a secondary maximum is observed near 27 °C. Then, from 27 to 38 °C, a decrease of the two moduli is observed. Finally, in the $38 \leq T \leq 60$ °C domain, a much weaker, continuous, and progressive decrease is observed as it was the case upon cooling. The values, slightly higher than those observed upon cooling since fat is known to be in the liquid state (cf DSC-7 results), refer to the reinforcement of the proteinic network leading to a more structured and strengthened product. On another hand, the gradual but limited changes in the elastic and viscous components in the range 40−60 °C can be interpreted according to Reparet and Noël (*11*) as specific of the mechanical resistance of the proteinic network.

The global decrease of G' modulus upon heating indicates a weakening of the cheese structure. The latter does not seem to be related to a destabilization of the fat matter since no "oiling off" or fat leakage was observed during rheological measurements even at high temperature. Moreover, no change in the microstructure of the fat droplets in processed cheese was observed upon heating of the sample during microscopic observations (result not shown).

The nonmonotonous behavior of the rheological parameters suggests that important and antagonist transformations occur

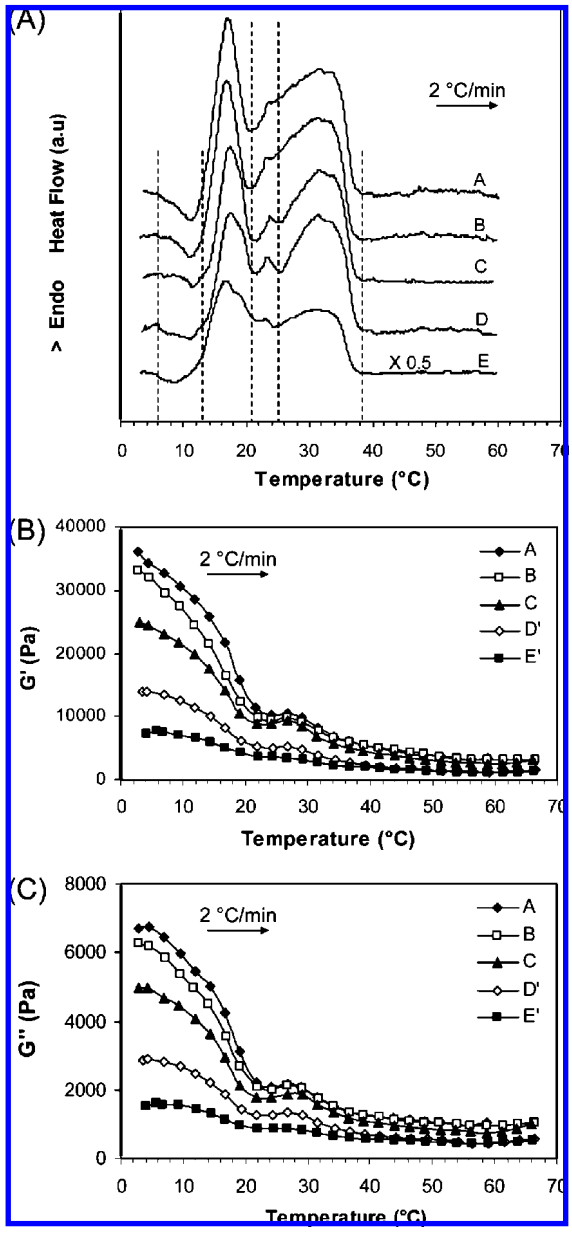

Figure 5. Evolution of (**A**) thermal and (**B** and **C**) viscoelastic properties of processed cheese during heating at 2 °C min^{-1} of the sample cheeses previously cooled down at (A) 0.5, (B) 1, (C) 2, (D) 5 (DSC-7), (D′) 4 (rheology), (E) 10 (DSC-7), and (E′) 6.5 °C min^{-1} (rheology).

at least in one component of the cheese. Determining which component is responsible for these changes represents one of the goals of the present work.

Relation between the Melting Behavior of Fat and the Viscoelastic Properties of Processed Cheese. To better understand the rheological properties of processed cheese upon heating, the latter have been correlated with the X-ray data. The procedure previously used upon cooling was applied again to analyze the characteristic diffraction lines. Thus, the intensity of the SAXD line has been determined through the detailed analysis of the individual frames.

The intensities of the XRD peaks of the 3L and 2L structures are reported in Figure **6**. Below 0 °C, the intensities of the three lines associated with the 3Lα (72 Å) remain constant. From 0 °C and up to 12−13 °C, the lowering of the intensities of all of the diffraction lines of this 3Lα structure is observed. This shows that the variations of G' and G'' moduli in the first above defined domain (3−12 °C) are due to the melting of the 3Lα crystals

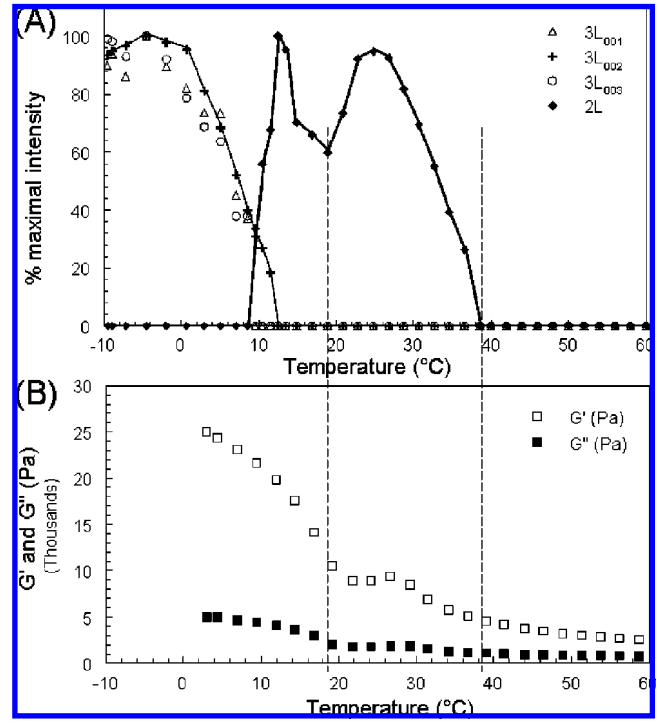

Figure 6. (**A**) Evolution of the maximal intensity of the XRD peaks recorded at small angles on heating of processed cheese at 2 °C min^{-1}. (**B**) Evolution of G' and G'' on heating at 2 °C min^{-1}, after cooling at the same rate.

embedded in the fat droplets. The following decrease of the viscoelastic parameters from 12 to 21 °C corresponds to the melting of the 2L (36.7 Å) structure, the formation of which does not much influence the rheology of the cheese since it coincides with the end of the melting of the 3Lα structure. Above 21 °C and up to 26 °C, the increase of G' and G'' is highly correlated to the formation of the 2L (40.6 Å) structure. Continuous variation of the peak position from 14 to 25 °C is not in contradiction with the successive decrease and increase of the viscoelastic parameters since a lowering of the SAXD intensity is first observed from 14 to 19 °C followed by an intensity increase from 19 up to 25 °C. The first behavior corresponds to the melting of the 2Lβ' phase from 14 to 22 °C and the second one to the formation of the 2L (40.6 Å) structure, which starts at about 12−16 °C and reaches a maximum at 25 °C. The different influences of these two structures of the TGs on the rheological moduli might explain the slight difference between the temperatures of the minimal intensity (19 °C) and that observed for G' and G'' (21 °C). Above 25 °C, melting of the 2L (40.6 Å) structure (and thus of all the TGs) present in the fat droplets is clearly responsible for the G' and G'' decrease observed up to the offset temperature of 38−40 °C.

The decrease of the G' and G'' moduli (**Figure 5B**,**C**) observed between 3 and 12−13 °C coincides with the first endotherm and the small exotherm of the DSC-7 recordings (**Figure 5A**) and with the 3Lα (72 Å) → 2L (36.7 Å) phase transition observed with the X-ray technique. The subsequent decrease of the rheological parameters between 13 and 21 °C is related to the major endotherm observed with both DSC-7 and DTA/XRDT calorimeters. X-ray data allowed us to attribute these changes to the transformation of the 2L (36.7 Å) into a 2Lβ' (40.6 Å) structure with a continuous variation of the peak position. The nonmonotonous variations of G' and G'' in the 21 to 38 °C temperature interval correspond to the broad

endotherm (observed with both calorimeters) associated to the melting of the 2L structure.

As a conclusion, the rheological, thermal, and structural properties that have been investigated in this study increased the understanding of the behavior of processed cheese in the temperature interval 3−60 °C. Although fat constitutes the dispersed phase, the influence of its crystallization, melting, and more generally its polymorphism upon the viscoelastic properties have been clearly demonstrated. Furthermore, the combination of small and wide angles XRD allowed us to identify the structures of the TGs in the fat droplets responsible for the rheological changes. Identification of these structures constitutes in itself a new and original study. Connection with rheological and thermal behaviors leads us to progress even further in understanding the physicochemical properties of processed cheeses. Such an approach is essential to go further in the analysis of the technofunctional and sensorial properties of food products and opens a new field of investigations.

ABBREVIATIONS USED

SAXD, small-angle X-ray diffraction; WAXD, wide-angle X-ray diffraction; XRDT, X-ray diffraction as a function of temperature.

ACKNOWLEDGMENT

We thank the Fromageries Bel (Vendôme, France) for supporting this research. H. Amenitsch (SAXS Beamline, synchrotron Elettra, Italy) is also acknowledged for beamline setup and collaboration in the X-ray diffraction experiments. We thank Dr. Sylviane Lesieur, Faculté de Pharmacie, Univ. Paris-Sud, and Professor Hamadi Attia, ENIS, Sfax, Tunisia, for their support as well as Dr. Valérie Nicolas, Plateau Technique de Microscopie Confocale, IFR 141, Faculté de Pharmacie, Univ. Paris-Sud, for her assistance in the CLSM experiments.

LITERATURE CITED

(1) Jensen, R. G.; Newburg, D. S. *Handbook of Milk Composition*; Jensen, R. G., Ed.; Academic Press: San Diego, CA, 1995.

(2) Timms, R. E. The phase behavior and polymorphism of milk fat, milk fat fractions, and fully hardened milk fat. *Aust. J. Dairy Technol.* **1980**, *35*, 47–53.

(3) Ollivon, M.; Perron, R. Propriétés physiques des corps gras. In *Manuel des Corps Gras*; Karleskind, A., Wolff, J. P., Guttmann, J. F., Eds.; Lavoisier: Paris, 1992; pp 433−503.

(4) Lee, S. K.; Buwalda, R. J.; Euston, S. R.; Foegeding, E. A.; McKenna, A. B. Changes in the rheology and microstructure of processed cheese during cooking. *Lebensm.-Wiss. Technol.* **2003**, *36*, 339–345.

(5) Subramanian, R.; Muthukumarappan, K.; Gunasekaran, S. Linear viscoelastic properties of regular- and reduced-fat pasteurized process cheese during heating and cooling. *Int. J. Food Prop.* **2006**, *9*, 377–393.

(6) Lopez, C.; Lesieur, P.; Bourgaux, C.; Keller, G.; Ollivon, M. Thermal and structural behavior of milk fat: 2. Crystalline forms obtained by slow cooling of cream. *J. Colloid Interface Sci.* **2001**, *240*, 150–161.

(7) Lopez, C.; Bourgaux, C.; Lesieur, P.; Bernadou, S.; Keller, G.; Ollivon, M. Thermal and structural behavior of milk fat. 3. Influence of cooling rate and droplet size on cream crystallization. *J. Colloid Interface Sci.* **2002**, *254*, 64–78.

(8) Lopez, C.; Lesieur, P.; Bourgaux, C.; Ollivon, M. Thermal and structural behavior of anhydrous milk fat. 3. Influence of cooling rate. *J. Dairy Sci.* **2005**, *88*, 511–526.

(9) Auty, M. A. E.; Twomey, M.; Guinee, T. P.; Mulvihill, D. M. Development and application of confocal laser scanning laser microscopy methods for studying the distribution of fat and protein in selected dairy products. *J. Dairy Res.* **2001**, *68*, 417–427.

(10) Lopez, C.; Briard-Bion, V. The composition, supramolecular organisation and thermal properties of milk fat: a new challenge for the quality of food products. *Lait* **2007**, *87*, 317–336.

(11) Reparet, J. M.; Noël, Y. Relation between a temperature-sweep dynamic shear test and functional properties of cheeses. *Lait* **2003**, *83*, 321–333.

(12) Horne, D. S.; Banks, J. M.; Leaver, J.; Law, A. J. R. Dynamic mechanical spectroscopy of Cheddar cheese. In *Cheese Yield and Factors Affecting Its Control*; Special issue 9402; Int. Dairy Fed.: Brussels, Belgium, 1993; pp 507−512.

(13) Ustunol, Z.; Kawachi, K.; Steffe, J. Arnott test correlates with dynamic rheological properties for determining cheddar cheese meltability. *J. Food Sci.* **1994**, *59*, 970–971.

(14) Tuckey, S. L.; Ruehe, H. A.; Clark, G. L. An X-ray diffraction analysis of cheddar cheese. *J. Dairy Sci.* **1938**, *21*, 777–789.

(15) Evans, E. W.; Pillinger, S. L. Examination of the structure of the bovine milk-fat-globule membrane and of cheese by X-ray crystallography. *J. Dairy Res.* **1973**, *40* (1), 17–27.

(16) Lopez, C.; Briard-Bion, V.; Beaucher, E.; Ollivon, M. Multiscale characterization of the organization of triglycerides and phospholipids in emmental cheese: From the microscopic to the molecular level. *J. Agric. Food Chem.* **2008**, *56* (7), 2406–2414.

(17) Scharpf, L. G., Jr.; Michnick, M. J. In situ identification of crystals on process cheese by X-ray diffraction. *J. Dairy Sci.* **1967**, *50* (12), 1989–1991.

(18) Caric, M.; Gantar, M.; Kalab, M. Effects of emulsifying agents on the microstructure and other characteristics of process cheese−A review. *Food Microstruct.* **1985**, *4*, 297–312.

(19) Lavigne, F. Polymorphisme et transitions dephase des triglycérides, applications aux propriétés thermiques et structurales de la matière grasse de lait anhydre et de ses fractions. Thesis, E.N.S.I.A., Massy, France, 1995.

(20) Lopez, C.; Briard-Bion, V.; Camier, B.; Gassi, J. Y. Milk fat thermal properties and solid fat content in emmental cheese: A differential scanning calorimetry study. *J. Dairy Sci.* **2006a**, *89*, 2894–2910.

(21) Lopez, C.; Maillard, M.-B.; Briard-Bion, V.; Camier, B.; Hannon, J. A. Lipolysis during ripening of Emmental cheese considering organization of fat and preferential localization of bacteria. *J. Agric. Food Chem.* **2006b**, *54*, 5855–5867.

(22) Famelart, M. H.; Le Graet, Y.; Michel, F.; Richoux, R.; Riaublanc, A. Evaluation des méthodes d'appréciation des propriétés fonctionnelles des fromages d'Emmenthal de l'Ouest de la France. *Lait* **2002**, *82*, 225–245.

(23) Michalski, M.-C.; Camier, B.; Briard, V.; Leconte, N.; Gassi, J.-Y.; Goudédranche, H.; Michel, F.; Fauquant, J. The size of native milk fat globules affects physico-chemical and functional properties of Emmental cheese. *Lait* **2004a**, *84*, 343–358.

(24) Rowney, M.; Roupas, P.; Hickey, M.; Everett, D. W. Milk fat structure and free oil in mozzarella cheese. *Aust. J. Dairy Technol.* **1998**, *53*, 110.

(25) Söderberg, I.; Hernqvist, L.; Buchheim, W. Milk fat crystallization in natural milk fat globules. *Milchwissenschaft* **1990**, *44*, 403–406.

(26) Michalski, M.-C.; Ollivon, M.; Briard, V.; Leconte, N.; Lopez, C. Native fat globules of different sizes selected from raw milk: Thermal and structural behavior. *Chem. Phys. Lipids* **2004b**, *132*, 247–261.

(27) Ollivon, M.; Keller, G.; Bourgaux, C.; Kalnin, D.; Villeneuve, P.; Lesieur, P. DSC and high resolution X-ray diffraction coupling. *J. Therm. Anal. Calorim.* **2006**, *85*, 219–224.

(28) Larsson, K. Molecular arrangement in glycerides. *Fette Seifen Anstrichm.* **1972**, *74*, 136–142.

(29) Lopez, C.; Bourgaux, C.; Lesieur, P.; Riaublanc, A.; Ollivon, M. Milk fat and primary fractions obtained by dry fractionation: 1. Chemical composition and crystallisation properties. *Chem. Phys. Lipids* **2006**, *144*, 17–33.

(30) Tunick, M. H. Effects of homogenization and proteolysis on free oil in mozzarella cheese. *J Dairy Sci*. **1994**, *77*, 2487–2493.
(31) Campos, R.; Narine, S. S.; Marangoni, A. G. Effect of cooling rate on the structure and mechanical properties of milk fat and lard. *Food Res. Int*. **2002**, *35*, 971–981.
(32) Zhong, Q.; Daubert, C. R.; Velev, O. D. Cooling effects on a model rennet casein gel system: Part I. Rheological characterization. *Langmuir* **2004**, *20*, 7399–7405.
(33) Guinee, T. P.; Caric, M.; Kalab, M. Pasteurized processed cheese and substitute/imitation cheese products, Major Cheese Groups. In *Cheese: Chemistry, Physics and Microbiology*; Fox, P. F., McSweeney, P. L. H., Cogan, T. M., Guinee, T. P., Eds.; Elsevier: San Diego, CA, 2004; Vol. 2, pp 349−394.
(34) Zhong, Q.; Daubert, C. R.; Farkas, B. E. Cooling effects on processed cheese functionality. *J. Food Process Eng*. **2004b**, *27*, 372–412.
(35) Caric, M.; Kalab, M. Processed cheese products. In *Cheese: Chemistry, Physics and Microbiology*; Fox, P. F., Ed.; Chapman and Hall: New York, 1993; Vol. 2, pp 467−505.
(36) Piska, I.; Stetina, J. Influence of cheese ripening and rate of cooling of the processed cheese mixture on rheological properties of processed cheese. *J. Food Eng*. **2004**, *61*, 551–555.
(37) Sanchez, C. Effets des traitements technologiques sur les caractéristiques rhéologiques et microstructurales d'une émulsion fromagère complexe. Thesis, Institut National Polytechnique de Lorraine, Nancy, France, 1994.

Received for review September 22, 2008. Revised manuscript received February 23, 2009. Accepted February 23, 2009. We are very indebted to Dr. Sylviane Lesieur, Faculté de Pharmacie, Univ. Paris-Sud, and Benoît Goldschmidt, Fromageries Bel, for their help concerning the grant for Hela Gliguem and for reading the manuscript.

JF802956B